Performance of DVR Using Optimized PI Controller Based Gradient Adaptive Variable Step LMS Control Algorithm

Naidu, Talada Appala; Arya, Sabha Raj; Maurya, Rakesh; Padmanaban, Sanjeevikumar

Published in:
IEEE Journal of Emerging and Selected Topics in Industrial Electronics

DOI (link to publication from Publisher):
10.1109/JESTIE.2021.3051553

Publication date:
2021

Document Version
Accepted author manuscript, peer reviewed version

Performance of DVR using Optimized PI Controller based Gradient Adaptive Variable Step LMS Control Algorithm

Talada Appala Naidu, *Member, IEEE,* Sabha Raj Arya, *Senior Member, IEEE,*
Rakesh Maurya, *Member, IEEE and* Sanjeevikumar Padmanabhan, *Senior Member, IEEE*

***Abstract*— A custom power device known as dynamic voltage restorer (DVR) has been investigated to operate a distribution system at its desired performance. The distribution system with voltage related power quality issues in the supply side have been addressed through this article using DVR. Four different grid disturbances such as voltage sag, swell, unbalances, and distortions have been taken into account while testing the DVR capability. DVR has been controlled using an optimized proportional and integral (PI) gains integrated with gradient adaptive variable learning rate least mean square control algorithm. Adaptiveness of variable step-size in LMS makes the control robust in case of dynamics in the system assures the better performance. Also, the other major contribution of this work is implementation of an optimization based self-tuning PI gains in proposed control. The evaluation of optimizer in estimating the PI gains is presented in terms of the response of DC-Link voltage DVR. The simulation work of proposed control algorithms on DVR has been done and found the satisfactory results. For the experimental validation d-SPACE made Micro Lab Box is used as control processor, both dynamic and steady state results are discussed for its effectiveness.**

***Key words*— Voltage Compensation, GAVS-LMS, DVR, PI controller, Sag, Unbalance.**

I. INTRODUCTION

As more devices or equipment are being used nowadays which creates power quality disturbances in the power system network frequently [1]. Differed Power Quality (PQ) issues degrade the response of connected power system equipment and further performance of the system. The voltage and current related PQ disturbances are widely seen problems with their possibility of occurrence and cause frequency [2]. The device which used to monitors these PQ problems under the standard limits are named as custom power devices. An elaborative study on these compensating devices has been reported with different configurations and topologies with their corresponding design aspects [3]. Some other new categorization of power quality problems is mentioned along with different PQ monitoring approaches [4].

Manuscript received on 25 July 2020; revised on 19 November 2020; accepted on 11 December 2020.
This work is supported by Science and Engineering Research Board –New Delhi (India) Research Project under Extra Mural Research Funding Scheme, Grant No. SB/S3/EEEC/030/2016, Dated 17/08/2016.
Talada Appala Naidu, Sabha Raj Arya and Rakesh Maurya are with Department of Electrical Engineering, Sardar Vallabhbhai National Institute of Technology, (SVNIT), Dumas Road, Surat-395007, India
(e-mail: naidu284@gmail.com, sabharaj1@gmail.com and rmaurya@eed.svnit.ac.in)
Sanjeevikumar Padmanabhan is with Department of Energy Technology, Aalborg University, Esbjerg 6700, Denmark (e-mail: san@et.aau.dk)

From this, it is found that the series connected custom power device can make sure of maintaining the voltage related PQ disturbances [6]. Mansoor *et al.* [7], have addressed the dynamic voltage restorer (DVR) as power quality improvement devices. Few numbers of configurations of DVR based on the topologies of voltage source converter (VSC) or energy storage element can be identified in recent literature with their operation [8-12]. A DVR with diode clamped inverter-based topology which is supported by a fuel cell for DC voltage has been investigated in [8]. In this system DVR is PQ monitoring device only whereas the main contribution is fuel cell-based DG system. A solid-state fault current limit-based DVR topology has been studied with a control such that it deactivates the DVR and activates the switches of DC link when fault occurs [9]. Sitharthan *et al.* [10] have proposed a DVR topology with customized hybrid control for the grid connected wind based distributed power generation using DFIG. Authors in text [11] have proposed a dual DC port DVR with a DC-DC converter support during the deep sag cases which reduces the capacity of DC-DC converter to half of the conventional ones. However, this research has addressed only the voltage sag in this which reduces the utilization of application of DVR which can also compensate few more PQ disturbances. Naidu *et al.* [12] have adapted a DVR configuration with self-supported DC-link capacitor as an energy storage element. Even though the proposed configuration is well known before, by applying a new control algorithm for controlling DVR it achieved an acceptable result in multi disturbances compensation.

In the view of enhancement of the performance of DVR, few out of several control algorithms have been identified [13-20]. Ye *et al.* [13] have proposed an elliptical restoration algorithm on single phase DVR in which the DVR injected voltage has been described in terms of the active and reactive components using virtual impedance of system. Authors in [14] have implemented DVR to enhance the power quality using the type 2 fuzzy logic controller. In this control adaptiveness has been utilized systems in the control domain to make DVR reliable for which a DC-DC converter has been implemented in topology. A sliding mode control (SMC) based control has been proposed to control DVR injected voltage for adjusting the terminal voltage of load to restore it to pre-sag value [15]. Hung *et al.* [16] have implemented DVR with two loop-based control algorithms. Out of two loops, external loop is of voltage which uses a decoupled resonant, other one is the inner loop which is of current and it uses the PR controller. Authors in [17] have been used the simple basic synchronous reference theory in the DVR for the compensation of any type

This article has been accepted for publication in a future issue of this journal, but has not been fully edited. Content may change prior to final publication. Citation information: DOI 10.1109/JESTIE.2021.3051553, IEEE Journal of Emerging and Selected Topics in Industrial Electronics

of voltage variations in the supply voltage. Alhaj *et al.* [18] have used the LMS based control for the approximation of magnitude and phase angle of harmonics in power system and compared it with Least Mean Fourth (LMF) and Least Mean Square/Fourth (LMS/F), it has been observed that the LMS/F produces the better results. In text [19], authors have dealt with a combination of LMS and LMF in the application distributed static compensator for getting active and reactive components of load voltage in forming the supply reference currents. Martins *et al.* [20] have proposed a control which relies on the construction of the voltage reference using the recursive least square (RLS) technique but is only suitable to harmonic distortions, sags, and swells.

As PI controller plays a vital role in role in DVR to compensate voltage-based PQ disturbances and to maintain the load voltage at the desired constant level. In this regard, authors in text [21] have proposed a self-tuned fuzzy controller type of PI regulators scheme for DVR control. The constraints in this method are to formulate the membership function which limits the application fuzzy logic-based PI in the systems such as custom power devices. The other way to tune the PI controllers' gains is the optimization methods which is an approximation approach in which, the system control algorithms will need less efforts due to the work of PI gains estimation has left to optimization method [12]. A gradient based adaptive step-size Least Mean Square (LMS) is used in this work [22]. In this filter, the change in step size is based on gradient descent algorithm which is designed so as to reduce squared estimation error in the process of each iteration that will ensure the better convergence. Due to adaptiveness of variable step-size in LMS, it makes the control robust in case of dynamics in the system which assures the better performance. For tuning of PI controllers in this work, a recent and simple optimization algorithm named as Rao1, Rao2, and Rao3 are implemented [23].

In this paper, authors have proposed an optimized PI gains based adaptive type of control algorithm for DVR of self-supported three phase VSC topology. The performance of these algorithms in estimation of PI gains has been compared in between them and presented here. These three optimization algorithms are simple to implement due to the fact that these algorithms only need size of the population and number of iterations other than any algorithm-specific control parameters. DVR performance using the proposed GAVS-LMS based control has been evaluated in MATLAB/Simulation platform. After obtaining the Simulation results, the proposed control algorithm has been evaluated on a scaled down system prototype of DVR using d-SPACE made Micro Lab Box processor. The simulation and experimental results of internals signals of the control along with the dynamic and steady state results of the DVR are presented.

II. DVR System Description

The self-supported DVR configuration that has been chosen for the voltage compensation is represented in Fig. 1. A non-ideal three phase ac grid is made by creating four types of loading conditions with different timing at same point. Four different loads are inductive load, capacitive load, unbalanced load, and rectifier load to create sag, swell, unbalances, and distortions respectively in the supply voltage.

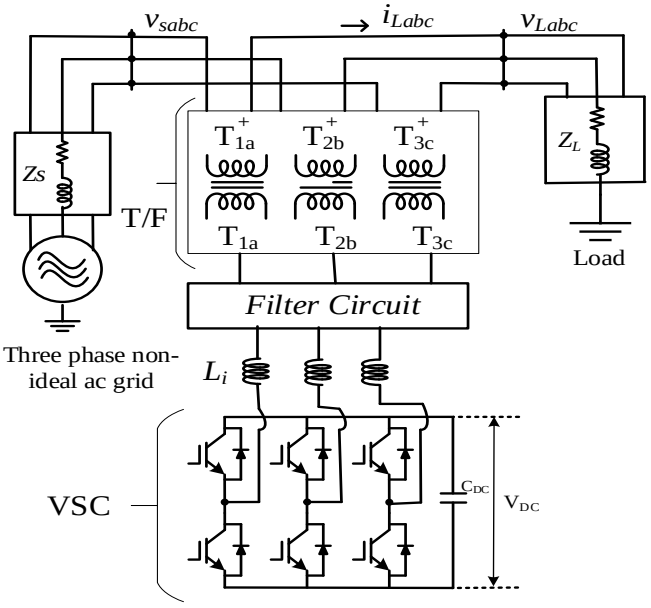

Fig. 1 DVR system configuration

The load that considered as the sensitive or critical load to be protected is linear load of RL for which it is to be maintained at constant Load voltage as shown in Fig. 1. The non-ideal ac supply system has been connected to sensitive load through injection transformers and voltage source converter as a DVR in supply system. As proposed, the system configuration is self-supported, the energy storage system has been replaced with capacitor "C_{dc}" which supports the voltage dynamics in the supply voltage when required using reactive power only. Therefore, active power transfer is not required as the compensation process has been done only by reactive power transfer. The switching harmonics generated by SVC has to be passed through filters "R_f, C_f" before injecting into the line. The interfacing inductors "L_i" have been employed for eliminating the current ripples of the converter. With suitable selection of transformation ratio and rating of the injection transformers based on the ratings of the load and supply voltage, the DVR system configuration can be made work suitably for compensation of listed issues in supply. The parameters selected for simulation work as well as experimental work are given in Appendix-A.

III. GAVS-LMS Control Algorithm

A Gradient Adaptive Variable Step-size LMS (GAVS-LMS) based control is implemented for DVR control. GAVS-LMS is used to estimate the fundamental active and reactive component of the supply voltage [22]. The supply voltage here is of disturbed in different aspects. So, the fundamental components have to be estimated out of this disturbed signal using GAVS-LMS in which the variable step size ($\gamma(n)$) is involved to make control robust for the system dynamics. The continuous estimation of variable step size has been found using eqn. (3). Fig. 2 shows the complete control algorithm using GAVS-LMS to generate the gate pulses to the switches of VSC. This figure includes the fundamental active component extraction unit and reactive components extraction unit, amplitude calculation of PCC voltage (V_{tA}) from which

This article has been accepted for publication in a future issue of this journal, but has not been fully edited. Content may change prior to final publication. Citation information: DOI 10.1109/JESTIE.2021.3051553, IEEE Journal of Emerging and Selected Topics in Industrial Electronics

the load reference voltage (v^*_{Labc}) can be generated. After the extraction of the fundamental components both active and reactive of each phase, these components have been averaged to find the fundamental components of three wire supply voltage. The process of estimation of load reference voltage for DVR control using GAVS-LMS based control can be seen in the following steps.

A. Fundamental Components Estimation using GAVS-LMS based Control

The details of the GAVS-LMS unit for fundamental estimation have been explained with help of equations and Fig.2. Eqn. (3) explains the step size "$\gamma(n)$" calculation for phase 'a', which provides the adaptiveness of the variable step size[22].

Here, "$u_{pa}(n)$" is unit template and a positive constant "ρ" that controls the adaptiveness of the step size. The weight update equations by GAVS-LMS algorithm is represented as (1), which can also be defined as the fundamental active part "W_{pa}" of the disturbed input signal.

$$W_{pa}(n+1)=W_{pa}(n)+\gamma_{pa}(n)\times e_{pa}(n)\times u_{pa}(n) \quad (1)$$

The error "$e_{pa}(n)$" between actual and estimated fundamental signals that has been computed using eqn. (2) for phase 'a' which is to be utilized in further control algorithm, where "v_{sa}" is supply voltage of phase 'a' and "$u_{pa}(n)$" in-phase unit template. The step size which varies with time has been represented with "$\gamma_{pa}(n)$" and derived using eqn. (3), unit templates used in this eqn. are calculated using eqns. (21, 22).

$$e_{pa}(n)=v_{sa}(n)-W_P^T(n)\times u_{pa}(n) \quad (2)$$

$$\gamma_{pa}(n)=\gamma_{pa}(n-1)+\rho\times e_{pa}(n)\times e_{pa}(n-1)\times u_{pa}^T(n-1)\times u_{pa}(n-1) \quad (3)$$

Similarly, active components with respect to non-ideal grid supply voltage of other two phase 'b' and 'c' as inputs are represented as "W_{pb}" and "W_{pc}" shown below.

$$W_{pb}(n+1)=W_{pb}(n)+\gamma_{pb}(n)\times e_{pb}(n)\times u_{pb}(n) \quad (4)$$

$$e_{pb}(n)=v_{sb}(n)-W_P^T(n)\times u_{pb}(n) \quad (5)$$

$$\gamma_{pb}(n)=\gamma_{pb}(n-1)+\rho\times e_{pb}(n)\times e_{pb}(n-1)\times u_{pb}^T(n-1)\times u_{pb}(n-1) \quad (6)$$

$$W_{pc}(n+1)=W_{pc}(n)+\gamma_{pc}(n)\times e_{pc}(n)\times u_{pc}(n) \quad (7)$$

$$e_{pc}(n)=v_{sc}(n)-W_P^T(n)\times u_{pc}(n) \quad (8)$$

$$\gamma_{pc}(n)=\gamma_{pc}(n-1)+\rho\times e_{pc}(n)\times e_{pc}(n-1)\times u_{pc}^T(n-1)\times u_{pc}(n-1) \quad (9)$$

Where "W_P" is the average of all three active components of supply voltage and calculated using eqn. (10).

$$W_P=Avg\{W_{pa},W_{pb},W_{pc}\} \quad (10)$$

In the same manner, fundamental reactive components with respect to disturbed supply voltage of three phases 'a, b, and c' are "W_{qa}", "W_{qb}", and "W_{qc}" as shown below.

$$W_{qa}(n+1)=W_{qa}(n)+\gamma_{qa}(n)\times e_{qa}(n)\times u_{qa}(n) \quad (11)$$

$$e_{qa}(n)=v_{sa}(n)-W_Q^T(n)\times u_{qa}(n) \quad (12)$$

$$\gamma_{qa}(n)=\gamma_{qa}(n-1)+\rho\times e_{qa}(n)\times e_{qa}(n-1)\times u_{qa}^T(n-1)\times u_{qa}(n-1) \quad (13)$$

$$W_{qb}(n+1)=W_{qb}(n)+\gamma_{qb}(n)\times e_{qb}(n)\times u_{qb}(n) \quad (14)$$

$$e_{qb}(n)=v_{sb}(n)-W_Q^T(n)\times u_{qb}(n) \quad (15)$$

$$\gamma_{qb}(n)=\gamma_{qb}(n-1)+\rho\times e_{qb}(n)\times e_{qb}(n-1)\times u_{qb}^T(n-1)\times u_{qb}(n-1) \quad (16)$$

$$W_{qc}(n+1)=W_{qc}(n)+\gamma_{qc}(n)\times e_{qc}(n)\times u_{qc}(n) \quad (17)$$

$$e_{qc}(n)=v_{sc}(n)-W_Q^T(n)\times u_{qc}(n) \quad (18)$$

$$\gamma_{qc}(n)=\gamma_{qc}(n-1)+\rho\times e_{qc}(n)\times e_{qc}(n-1)\times u_{qc}^T(n-1)\times u_{qc}(n-1) \quad (19)$$

Where "W_Q" is the average of all three reactive components of supply voltage and calculated using (20).

$$W_Q=Avg\{W_{qa},W_{qb},W_{qc}\} \quad (20)$$

Equation (21) and (22) are to find the unit templates that have been used in extracting the fundamental components where the magnitude (I_{Lm}) of load current is calculated using (23).

$$u_{pa}(n)=\frac{i_{La}}{I_{Lm}};u_{pb}(n)=\frac{i_{Lb}}{I_{Lm}};u_{pc}(n)=\frac{i_{Lc}}{I_{Lm}} \quad (21)$$

$$u_{qa}(n)=\frac{u_{pb}(n)-u_{pc}(n)}{\sqrt{3}};u_{qb}(n)=\frac{3u_{pb}(n)+u_{pb}(n)-u_{pc}(n)}{2\sqrt{3}};u_{qc}(n)=\frac{-3u_{pb}(n)+u_{pb}(n)-u_{pc}(n)}{2\sqrt{3}} \quad (22)$$

$$I_{Lm}=\sqrt{0.67\times\left(i_{La}^2+i_{Lb}^2+i_{Lc}^2\right)} \quad (23)$$

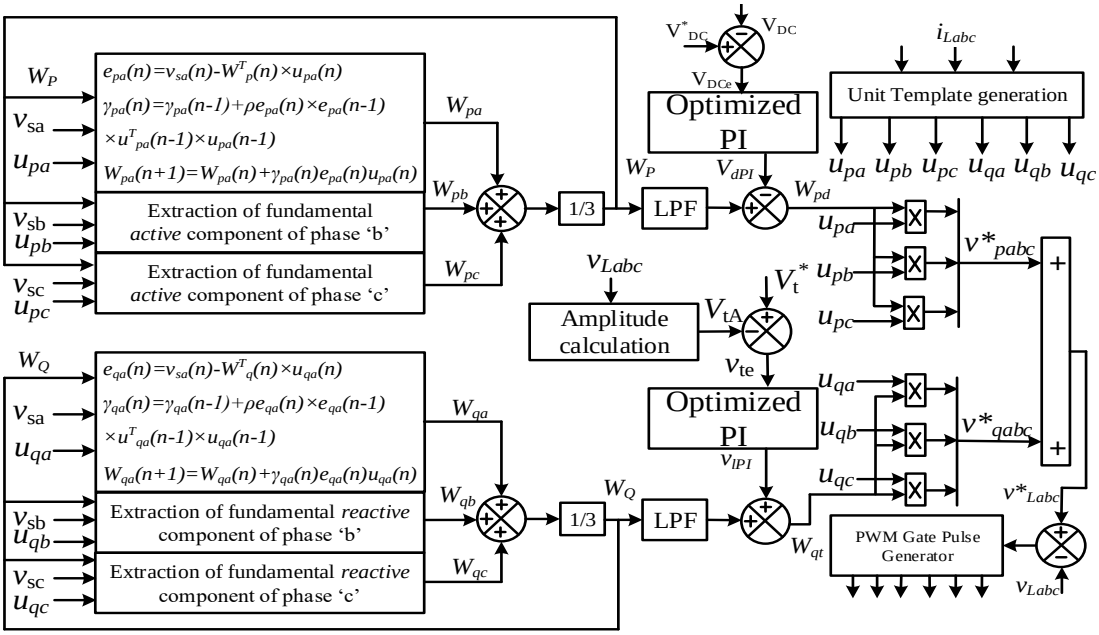

Fig. 2. Control algorithm for DVR using GAVS-LMS

B. Reference Load Voltage Computation and Gate Pulse Generation

After extracting the fundamental active "W_P" and reactive "W_Q" components of non-ideal supply grid voltage, the components of load voltage "v_{Lp}" and "v_{Lq}" has been calculated using (24).

$$v_{Lp} = W_P - v_{dPI}$$
$$v_{Lq} = W_Q + v_{lPI} \quad (24)$$

where v_{dPI} and v_{lPI} are output of DC and AC bus PI controller. Active as well as reactive component of load reference voltage are calculated by multiplying "v_{Lp}" and "v_{Lq}" with unit templates respectively as shown in (25). Finally, by adding active and reactive load reference voltages corresponding phases respectively, the reference load voltages (v^*_{Labc}) have been computed using (26).

$$v^*_{Lp} = v_{Lp} \times u_{pabc}$$
$$v^*_{Lq} = v_{Lq} \times u_{qabc} \quad (25)$$

$$v^*_{La} = v^*_{Lpa} + v^*_{Lqa}; v^*_{Lb} = v^*_{Lpb} + v^*_{Lqb}; v^*_{Lc} = v^*_{Lpc} + v^*_{Lqc} \quad (26)$$

Reference load voltages (v^*_{Labc}) and sensed load voltage (v_{Labc}) are compared then the error is processed through high frequency PWM pulse generator [3, 19]. These pulses have been given to three phase three leg VSC working as DVR for compensating the voltage related PQ disturbances. The successful implementation of pulse generation using GAVS-LMS based control algorithms ensures that the DVR compensates all the mention power quality disturbances which can be observed in the following sections.

IV. Simulation Based Results

The software simulation platform, MATLAB has been utilized for simulating the three-phase VSC based DVR with 'ode4' solver and 10 µsec sampling time. The gate pulses generated with 8 kHz frequency using GAVS-LMS based control have been processed to the VSC, so as to work as DVR for compensation of different disturbances in the supply. Three phase system is considered of having the voltage related issues in the supply side by associating different loads at the same supply bus. Voltage sag, swell, voltage distortions, and imbalances in the voltages have been included in the supply side. The performance of the GAVS-LMS based control as well as of the DVR have been studied and presented in this section as follows. It includes the reference load voltage generation and overall compensation capability of DVR with different voltage-based PQ problems. Also, for observing the performance of particular control algorithm on DVR, the time response has been analyzed during the compensation of unbalances in the supply grid voltage which has been explained in detail.

A. Performance of DVR using GAVS-LMS based control

Figure 3 (a) represents the dynamic performance of DVR using the proposed control for the mitigation of voltage-based power quality interruption. The voltage sag/swell, harmonics, and unbalance in the supply voltage (v_{sabc}) are considered for observing the dynamic performance as shown in subplot (1) of this figure. The compensating voltages (v_{cabc}) of three phases can be seen in subplots (2) to subplot (4) in this Fig. 3 (a). Therefore, after compensation using DVR, the load voltage (v_{Labc}) after compensated by DVR can be seen without any disturbances as shown in subplot (5) of the figure. The load current (i_{Labc}) is shown in subplot (6) of Fig. 3 (a). The load voltage amplitude (V_t) and the voltage across the DC-link (V_{DC}) can be seen at their reference values as presented in subplots (7-8). From Fig. 3 (a), it is understood that, the DVR using proposed GAVS-LMS based control algorithm has mitigated the disturbances in the load voltage.

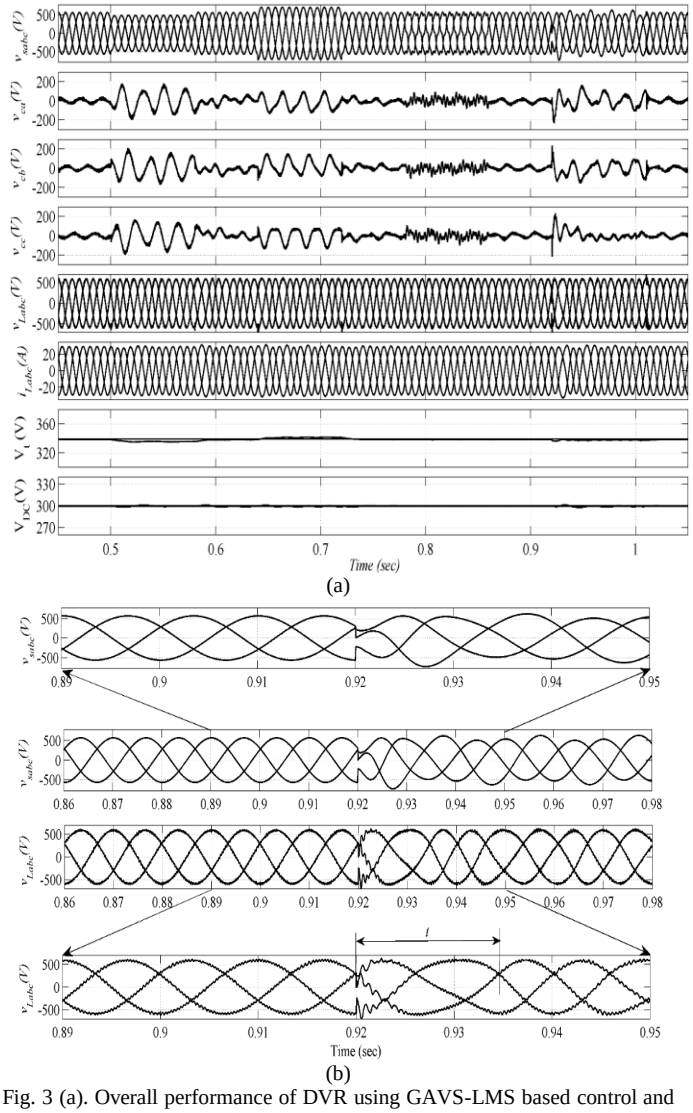

Fig. 3 (a). Overall performance of DVR using GAVS-LMS based control and (b)Time response of DVR in an unbalance compensation in supply using GAVS-LMS based control algorithm

Another side, the DVR capability has been evaluated in particular time response point of view in compensating the unbalances in the supply voltage. Fig. 3 (b) shows the time response of DVR while compensating one of the mentioned problems say unbalances in the supply voltage with developed control. In this figure, supply as well as load voltages are presented for the same duration. From the Fig. 3 (b), it is seen that DVR using GAVS-LMS control is able to suppress imbalances in the supply within 3/4th cycle. However, it is also to be understood that the remaining power quality problems can also found compensated using DVR within less time.

This article has been accepted for publication in a future issue of this journal, but has not been fully edited. Content may change prior to final publication. Citation information: DOI 10.1109/JESTIE.2021.3051553, IEEE Journal of Emerging and Selected Topics in Industrial Electronics

Fig. 4 shows the harmonic analysis during harmonics in the supply. Fig. 4 (a-c) shows the supply voltage (v_{sa}) with distortions, distortions free load voltage (v_{La}), and load current (i_{La}) of phase 'a' respectively. This figure also gives the details of their harmonic spectra in terms of Total Harmonic Distortions (THD). Fig. 4 (a) shows supply voltage which holds the harmonics of 9.78 % THD with a voltage of 538.7 V. After mitigation of distortions from supply voltage, load voltage is seen of 2.51 % THD with voltage of 586.4 V as shown in Fig. 4 (b). Fig. 4 (c) gives the information of load current of 1.22 % THD and current of 29.41A. The results obtained using DVR with proposed GAVS-LMS control algorithms are under the limits of IEEE Std. 519-2014.

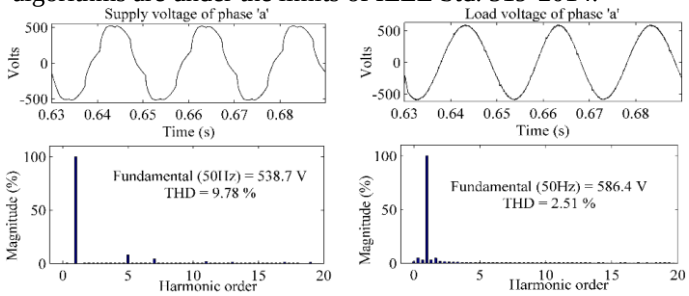

(a) supply voltage (v_{sa}) and its THD

(b) Load voltage (v_{La}) and its THD

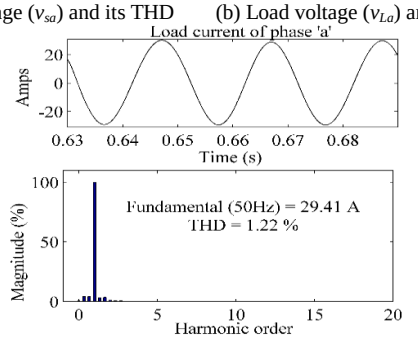

(c) Load current (i_{La}) and its THD

Fig. 4. Performance of DVR during steady state while distortions present in supply.

B. PI Controller Gains Estimation

PI controller tuning process has adapted a new method in this control that is an optimization of PI control gains. For this purpose, a recently developed optimization algorithms as "Rao algorithms" have been implemented in this control [23]. These optimization algorithms are simple in point of implementation for researchers due to the elimination of tuning burden of algorithm-specific parameters. The best and the worst solutions and the random interconnections between candidate solutions are basic requirements of these algorithms. The basic equations for Rao1, Rao2, and Rao3 are given below as eqn. (27), eqn. (28), and eqn. (29) respectively.

$$X^{n+1}_{j,k,i} = X^{n}_{j,k,i} + rand() \times \left[X^{n}_{j,b,i} - X^{n}_{j,w,i} \right] \quad (27)$$

$$X^{n+1}_{j,k,i} = X^{n}_{j,k,i} + rand_1() \times \left[X^{n}_{j,b,i} - X^{n}_{j,w,i} \right] + rand_2() \times \left[\left| X^{n}_{j,k,i} \text{ or } X^{n}_{j,l,i} \right| - \left| X^{n}_{j,l,i} \text{ or } X^{n}_{j,k,i} \right| \right] \quad (28)$$

$$X^{n+1}_{j,k,i} = X^{n}_{j,k,i} + rand_1() \times \left[X^{n}_{j,b,i} - \left| X^{n}_{j,w,i} \right| \right] + rand_2() \times \left[\left| X^{n}_{j,k,i} \text{ or } X^{n}_{j,l,i} \right| - \left(X^{n}_{j,l,i} \text{ or } X^{n}_{j,k,i} \right) \right] \quad (29)$$

Where, "$X^{n}_{j,b,i}$" is the best solution of the variable 'j' and "$X^{n}_{j,w,i}$" is the worst solution value of the variable 'j' during the i^{th} iteration. "$X^{n+1}_{j,k,i}$" is the updated value of "$X^{n}_{j,k,i}$" and *rand(), rand₁(), rand₂()* are random variables for j^{th} variable during i^{th} iteration.

The objective function is to estimate the gains of PI controllers by making actual signal equal to reference signal which mathematically modelled using eqn. (30).

$$F_{objective} = \int \left\{ t \times e^2 \right\} dt \quad (30)$$

Where *'e'*, the error between the reference and actual DC bus signal. Three Rao algorithms have been investigated in case of DC-link voltage and load voltage terminal magnitude tuning process. As four variables (gains of two PI controllers) are to be optimized the dimension '*k*' of variable is set to 4. The number of particles/candidates' '*j*' and number of iterations '*i*' are set to 50 and 10 after number of observations.

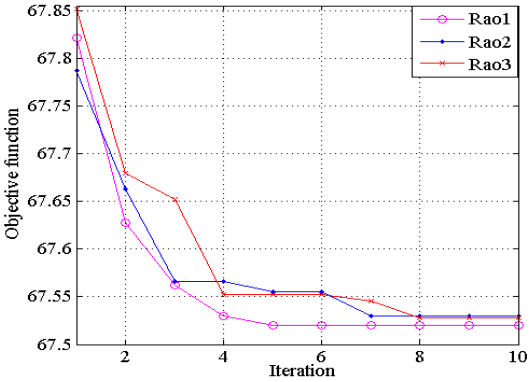

Fig. 5. Variation of objective function with respect to iterations

With the same specifications, three optimization algorithms have been implemented on the DVR system, to estimate the PI controller gains. DC-PI controller gains are named as k_{p1}, k_{i1}, whereas AC-PI gains are named as k_{p2}, k_{i2}. Table-1, Table-2, and Table-3 presents the values of PI gains k_{p1}, k_{i1}, k_{p2}, and k_{i2} with respect to iterations of Rao1, Rao2, and Rao3 algorithms respectively. From these tables, it is found that Rao1 algorithm is producing the constant values of variable (PI gains) form 5th iteration itself whereas Rao2 and Rao3 algorithms are producing at 7th and 8th iterations respectively. This can be witnessed in Fig. 5 that the objective functions of Rao1, Rao2, and Rao3 are getting settled at 5th, 7th, and 8th interactions respectively.

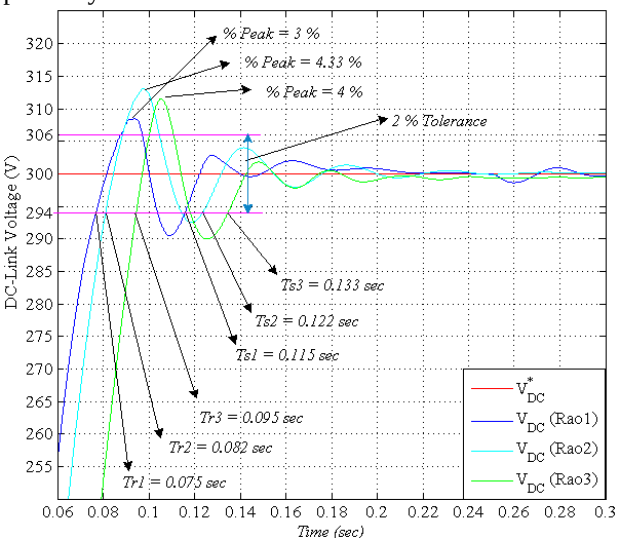

Fig. 6. DVR DC-Link voltage response with PI optimized with Rao1, Rao2, and Rao3 optimization algorithms

This article has been accepted for publication in a future issue of this journal, but has not been fully edited. Content may change prior to final publication. Citation information: DOI 10.1109/JESTIE.2021.3051553, IEEE Journal of Emerging and Selected Topics in Industrial Electronics

TABLE: 1. PI CONTROLLER GAINS OBTAINED BY RAO1 OPTIMIZATION

Variables to be optimized		Current Iteration									
		1	2	3	4	5	6	7	8	9	10
DC-PI controller	k_{p1}	1.261	1.653	1.254	1.254	1.254	1.254	1.254	1.254	1.254	1.254
	k_{i1}	0.270	0.356	0.279	0.236	0.236	0.236	0.236	0.236	0.236	0.236
AC-PI controller	k_{p2}	25.774	24.865	25.746	25.642	25.642	25.642	25.642	25.642	25.642	25.642
	k_{i2}	0.465	0.499	0.413	0.426	0.542	0.542	0.542	0.542	0.542	0.542

TABLE: 2. PI CONTROLLER GAINS OBTAINED BY RAO2 OPTIMIZATION

Variables to be optimized		Current Iteration									
		1	2	3	4	5	6	7	8	9	10
DC-PI controller	k_{p1}	1.236	1.634	1.686	1.212	1.236	1.254	1.254	1.254	1.254	1.254
	k_{i1}	0.635	0.236	0.964	0.125	0.264	0.369	0.236	0.236	0.236	0.236
AC-PI controller	k_{p2}	23.694	25.635	25.965	28.635	24.635	27.968	27.968	27.968	27.968	27.968
	k_{i2}	0.4103	0.4103	0.4103	0.4103	0.3713	0.3713	0.438	0.438	0.438	0.438

TABLE: 3. PI CONTROLLER GAINS OBTAINED BY RAO3 OPTIMIZATION

Variables to be optimized		Current Iteration									
		1	2	3	4	5	6	7	8	9	10
DC-PI controller	k_{p1}	1.236	1.634	1.686	1.212	1.236	1.254	1.254	1.254	1.254	1.254
	k_{i1}	0.635	0.236	0.964	0.125	0.264	0.369	0.236	0.236	0.236	0.236
AC-PI controller	k_{p2}	23.694	25.635	25.965	28.635	24.635	27.968	27.968	27.968	27.968	27.968
	k_{i2}	0.4103	0.4103	0.4103	0.4103	0.3713	0.3713	0.438	0.438	0.438	0.438

To examine the performance of PI controller with three optimization-based algorithms, the DC-link voltage PI controller tuning these three optimization algorithms is presented in Fig. 6. After the estimation of values of gains of PI that are to be applied in the developed control for necessary performance of the three-phase DVR. The DC link voltage response at the transient period. It is made that; the settling time of DC-Link voltage has been considered in the range of 2 % tolerance of 300 V (i.e. 294 V to 306 V). Rise time (T_r) has been calculated at 100% of final value. In Fig. 6, it can be observed that the performance of Rao1, Rao2, and Rao3 algorithms are presented with respect to rise time, settle time, and % of peak. It is seen that the DC-PI values produced by Rao1 are giving good time response as compared to other two algorithms.

V. EXPERIMENTAL RESULTS

The DVR prototype of scaled down parameters has been made in the laboratory with the help of d-SPACE (Micro Lab Box processor at sampling time of 30 µ.sec. The LEM made voltage (LV-25P) and current sensors, (LA-55P) are for sensing the grid voltages and currents at various points in the experimental setup. A four channel, DSOX2004A is used to record the dynamic results while compensation of the voltage disturbances. Fluke-43B, PQ analyzer has been used to record results in case of distortions in the supply voltage. Experimental results of DVR with GAVS-LMS based control algorithms are presented during sag and distortions in the supply voltage. However, the internal signals of the GAVS-LMS based control for reference load voltage generation is shown in case of sag in the supply voltage.

A. Experimental Performance of GAVS-LMS control

The performance of GAVS-LMS based control algorithms in generating the load reference voltage (v^*_{La}) of phase 'a' has been demonstrated in this subsection. The required internal signals of GAVS-LMS based control are presented in case of voltage sag in the supply voltage in Fig. 7. In Fig.7 (a) supply voltage of phase 'a' (v_{sa}), in-phase unit templates (u_{pa}), variable step size (γ_{pa}), and fundamental active component of phase 'a' (W_{pa}) are presented. Fig. 7 (b) shows the supply voltage of phase 'a' (v_{sa}), quadrature unit templates (u_{qa}), variable step size for reactive component (γ_{qa}), and fundamental reactive component of phase 'a' (W_{qa}). Fig. 7 (c) shows the supply grid voltage of phase 'a' v_{sa}, γ_{pa}, W_{pa} and W_{qa} in which the variations can be observed during the sag in the supply voltage. Fig. 7 (d) shows the reference DC-link voltage (V^*_{DC}) with its actual (V_{DC}) and load voltage terminal value (V^*_t) with its actual value (V_t) for comparison and it is seen that, both DC-link voltage and load terminal voltage are maintained at their rated reference value.

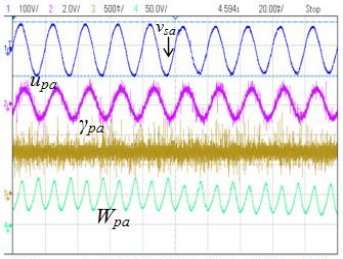

(a) In y-axis Ch1: 100V/div, Ch2: 1V/div, Ch3: 0.5V/div, Ch4: 50V/div and in x-axis 20ms/div

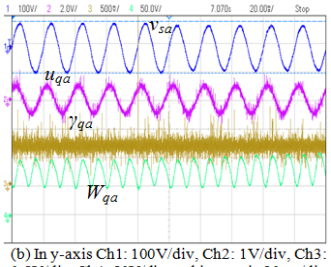

(b) In y-axis Ch1: 100V/div, Ch2: 1V/div, Ch3: 0.5V/div, Ch4: 50V/div and in x-axis 20ms/div

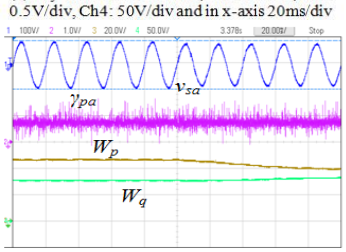

(c) In y-axis Ch1: 100V/div, Ch2: 1V/div, Ch3: 20V/div, Ch4: 50V/div and in x-axis 20ms/div

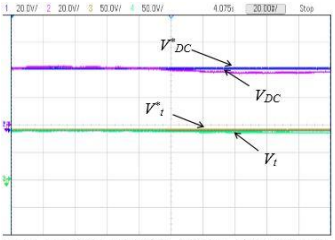

(d) In amplitude-axis Ch1,2: 20V/div, Ch3,4: 50V/div and in x-axis 20ms/div

This article has been accepted for publication in a future issue of this journal, but has not been fully edited. Content may change prior to final publication. Citation information: DOI 10.1109/JESTIE.2021.3051553, IEEE Journal of Emerging and Selected Topics in Industrial Electronics

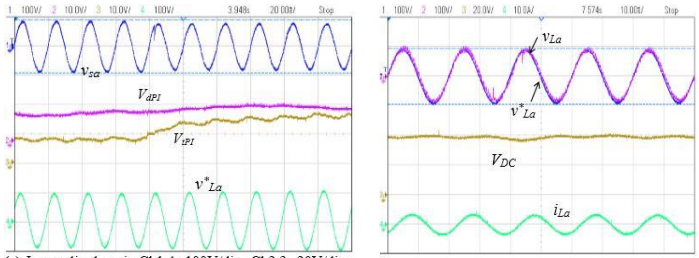

(e) In amplitude-axis Ch1,4: 100V/div, Ch2,3: 20V/div and in x-axis 20ms/div

(f) In amplitude-axis Ch1,2: 100V/div, Ch3: 20V/div, Ch4: 10 A/div and in x-axis 10ms/div

Fig. 7. Internal signals of GAVS-LMS based control in case of sag in supply voltage (a) v_{sa}, u_{pa}, γ_{pa}, W_{pa} (b) v_{sa}, u_{qa}, γ_{qa}, W_{qa} (c) v_{sa}, γ_{pa}, W_p, W_q (d) V^*_{DC}, V_{DC}, V^*_t, V_t (e) v_{sa}, V_{dPI}, V_{tPI}, v^*_{La} (f) v^*_{La}, v_{La}, V_{DC}, i_{La}

The reference load voltage (v^*_{La}) with outputs of DC-PI and ac-PI controllers (V_{dPI}) and (V_{tPI}) along with supply voltage of phase 'a' (v_{sa}) are reported in Fig. 7 (e). Load voltage tracking has been presented during the sag in the supply voltage of phase 'a' in Fig. 7 (f) for showing the effectiveness of developed control. The load reference voltage (v^*_{La}), sensed load voltage (v_{La}), DC-bus voltage (V_{DC}), and load current (i_{La}) have been included in this figure. From Fig.7, it is found that, the reference load voltage has been generated in case of sag in the supply using proposed control algorithm, however, it is to be noted that during remaining disturbances also proposed control is able to generate the reference signal at desired level for the operation of DVR.

B. Dynamic Performance of DVR with GAVS-LMS

The dynamic results of DVR system with GAVS-LMS control are presented to validate the control. Fig. 8-9 shows the voltage sag and harmonics compensation respectively using DVR with GAVS-LMS based control algorithm.

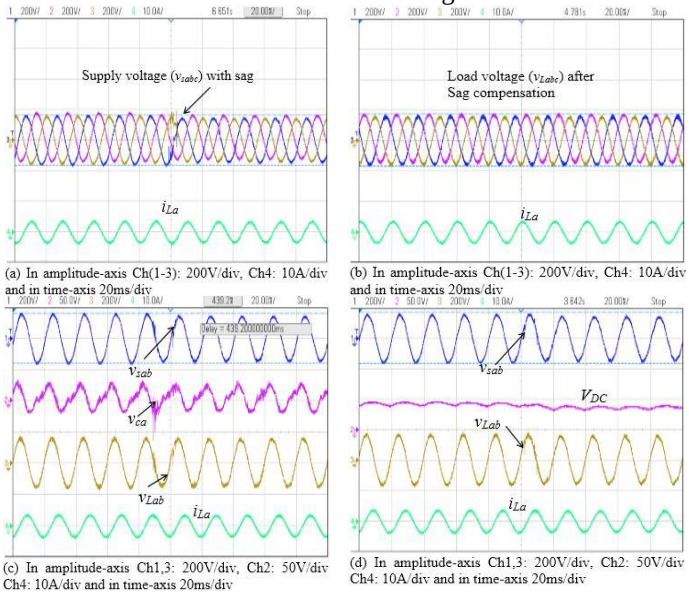

(a) In amplitude-axis Ch(1-3): 200V/div, Ch4: 10A/div and in time-axis 20ms/div

(b) In amplitude-axis Ch(1-3): 200V/div, Ch4: 10A/div and in time-axis 20ms/div

(c) In amplitude-axis Ch1,3: 200V/div, Ch2: 50V/div Ch4: 10A/div and in time-axis 20ms/div

(d) In amplitude-axis Ch1,3: 200V/div, Ch2: 50V/div Ch4: 10A/div and in time-axis 20ms/div

Fig. 8. Performance of three phase DVR for compensation of voltage Sag using GAVS-LMS control (a) v_{sabc}, i_{La} (b) v_{Labc}, i_{La} (c) v_{sa}, v_{ca}, v_{La}, i_{La} (d) v_{sa}, V_{DC}, v_{La}, i_{La}

The sag is created in supply voltage (v_{sabc}) as shown in Fig. 8 (a) and its corresponding load voltage (v_{Labc}) after compensation is set back to its desired value i.e. 110 V RMS as shown in Fig. 8 (b). Fig. 8 (c) illustrates the supply voltage (v_{sa}), compensating voltage (v_{cc}), load voltage (v_{La}), and load current (i_{La}) of phase 'a' which gives the clear picture of sag compensation. Fig. 8 (d) shows the supply voltage (v_{sa}), load voltage (v_{La}), load current (i_{La}) of phase 'a' and dc-Link (V_{DC}). Fig. 9 shows the mitigation of voltage distortions in the supply voltage. Distortions are created in supply voltage (v_{sabc}) as shown in Fig. 9 (a) and its corresponding load voltage (v_{Labc}) after compensation is set back to its desired value i.e 110 V RMS without any distortions in it as shown in Fig. 9 (b). Fig. 9 (c) shows the supply voltage (v_{sa}), compensating voltage (v_{cc}), load voltage (v_{La}), along with load current (i_{La}) of phase 'a' which gives the clear picture of distortions compensation. Fig. 9 (d) reveals the supply voltage (v_{sa}), load voltage (v_{La}), load current (i_{La}) of phase 'a', and DC-Link (V_{DC}) for the verification of DC-link voltage during the compensation. After observing these results, while compensating the PQ disturbances in the supply voltage, V_{DC} is also retained at reference level with effective dynamical response.

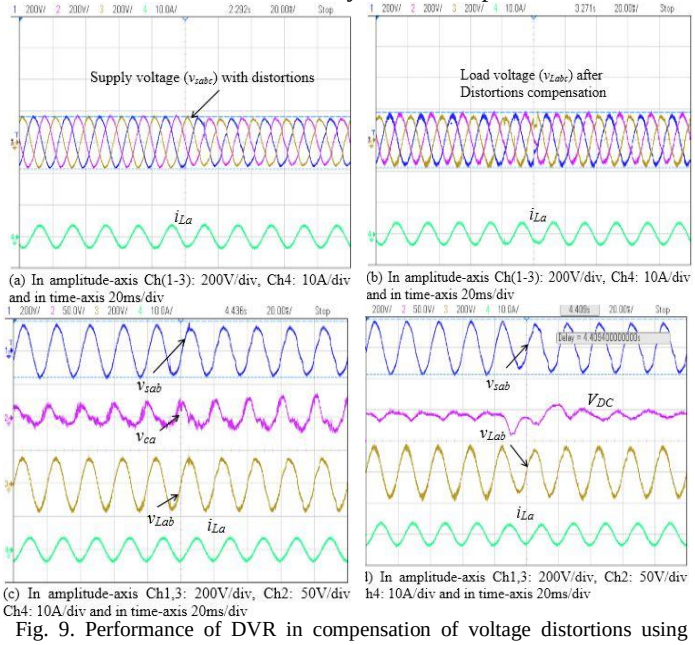

(a) In amplitude-axis Ch(1-3): 200V/div, Ch4: 10A/div and in time-axis 20ms/div

(b) In amplitude-axis Ch(1-3): 200V/div, Ch4: 10A/div and in time-axis 20ms/div

(c) In amplitude-axis Ch1,3: 200V/div, Ch2: 50V/div Ch4: 10A/div and in time-axis 20ms/div

(d) In amplitude-axis Ch1,3: 200V/div, Ch2: 50V/div Ch4: 10A/div and in time-axis 20ms/div

Fig. 9. Performance of DVR in compensation of voltage distortions using GAVS-LMS control (a) v_{sabc}, i_{La} (b) v_{Labc}, i_{La} (c) v_{sab}, v_{ca}, v_{Lab}, i_{La} (d) v_{sab}, V_{DC}, v_{Lab}, i_{La}

C. Performance of DVR during Harmonics Compensation

The work of DVR during steady state has been studied when the supply voltage includes with distortions and it is illustrated in Fig. 10. Fig. 10 (*a*) presents the supply grid voltage (v_{sa}) with distortions in it with load current (i_{La}). The THD is approximately 8 % which has been measured for supply voltage which is presented in Fig. 10 (*b*). Fig. 10 (c) shows load voltages (v_{La}) with load current (i_{La}). The THD value of 4.4% which has been measured for three phase load voltages which are presented in Fig. 10 (*d*). The compensated voltage of phase 'a' has been given in Fig. 10 (e). Fig 10 (f) gives the details of load current (i_{La}) of phase '*a*' and it's THD. The Steady state performance of DVR in other phases can also be found in Table-4 which are found satisfactory. It is seen that, after distortions mitigations the load voltage and load current are found to be under the limits of IEEE-519 Standards.

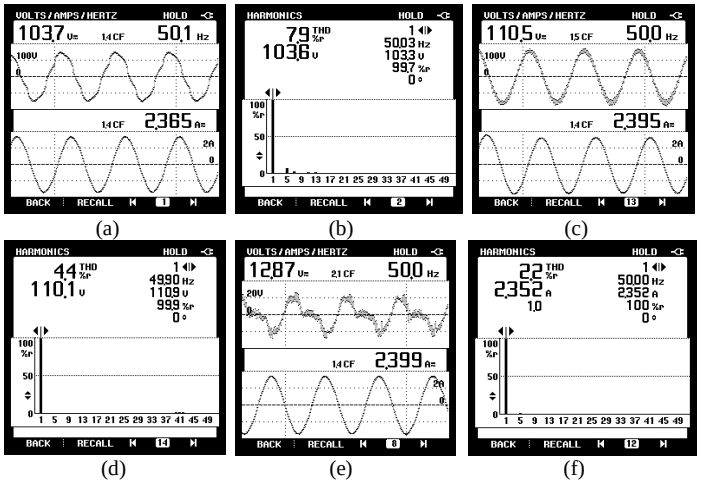

Fig.10. Performance of DVR during distortions in the supply voltage (*a*) supply voltage (v_{sab}) and load current (i_{La}) (*b*) THD of v_{sab} (c) load voltage (v_{Labc}) and load current (i_{La}) (*d*) THD of v_{Lab} (e) compensating voltage (v_{ca}) and (f) THD of load current (i_{La})

TABLE: 4. EXPERIMENTAL STEADY STATE RESULTS OF DVR

Sr. No.	Parameter	Value, %THD
1.	Supply voltage (v_{sab})	103.7 V, 7.9 %
2.	Supply voltage (v_{sbc})	101.5 V, 8.1 %
3.	Supply voltage (v_{sca})	103.9 V, 7.6 %
4.	Load voltage (v_{Lab})	110.5 V, 4.4 %
5.	Load voltage (v_{Lbc})	110.4 V, 4.4 %
6.	Load voltage (v_{Lca})	110.6 V, 4.6 %
7.	Load current (i_{La})	2.35 A, 2.2 %

VI. CONCLUSIONS

This paper discussed voltage-based PQ issues in three wire distribution networks with respect to voltage in the supply side using Dynamic Voltage Restorer. To assess the DVR performance four different disturbances viz. voltage sag, swell, unbalances, and distortions have been considered in the supply voltage. For controlling DVR in this regard, a GAVS-LMS based control algorithm using an optimized PI gains has been studied. The performances of three optimization algorithms have been studied compared in terms of time response of DC-Link voltage. It is found that Rao1 is producing the best values of PI gains within 5 iterations compared to other two algorithms which are taking 7 and 8 iterations respectively. The proposed control algorithms on DVR has been simulated and found the satisfactory performance in dynamic and steady state. An experimental validation of control has been done on DVR prototype which uses the d-SPACE made Micro Lab Box as control processor and found the results satisfactory. Both dynamic and steady state experimental results of DVR have been shown in this paper. The robustness of proposed control algorithm during the dynamics in the system has been achieved both in simulation and experimental results as well.

APPENDIX-A

A1. Parameters of three-phase VSC based DVR system for Simulation Work

Non-ideal grid supply -415 V, 50 Hz; Load of 15KVA with 0.8 p.f. (Lagg.); Load current (i_L) = 20.86 A; Injection-transformer: 3 kVA, 200/100 V; DC link voltage (V_{dc}) =300 V; DC bus capacitor (C_{dc})=3300 µ.F; and interfacing inductor (L_f)=1 mH; Ripple filter components: R_f = 6Ω and C_f=10 µF, Switching frequency (f_s) =8 kHz, Cut-off frequency (f_c) of LPF at DC link and load voltage bus = 10Hz, Sampling time (t_s)=10 µsec.

A2. Parameters of three-phase VSC based DVR system for Experimental Work

Non-ideal grid supply -110 V, 50 Hz; Load of 0.5 KVA; Load current (i_L) = 2.36 A; Rating of injection or DVR transformer: 4 kVA, 65/65 V; DC bus voltage (V_{dc})= 40 V; DC bus capacitor (C_{dc})= 4700 µ.F; and interfacing inductor (L_f)= 2 mH; Ripple filter components: R_f =10Ω and C_f= 40 µF, Sampling time (t_s)=30 µsec.

REFERENCES

[1] Math HJ. Bollen, *Understanding Power Quality Problems: In Voltage sags and Interruptions*, IEEE press, 2000.

[2] Arindam Ghosh and Gerard Ledwich, *Power Quality Enhancement Using Custom Power Devices*, Springer Science & Business Media, Dec. 2012.

[3] Bhim Singh, Ambrish Chandra, and Kamal Al-Haddad, *Power Quality: Problems and Mitigation Techniques*, John Wiley & Sons, 2014.

[4] Okan Ozgonenel, Turgay Yalcin, Irfan Guney, and Unal Kurt, "A new classification for power quality events in distribution systems," *Journal of Electric Power Systems Research*, vol. 95, pp. 192-199, Feb. 2013.

[5] Yahya Naderi, Seyed Hossein Hosseini, Saeid Ghassem Zadeh, Behnam Mohammadi-Ivatloo, Juan C. Vasquez, and Josep M. Guerrero, "An overview of power quality enhancement techniques applied to distributed generation in electrical distribution networks," *Renewable and Sustainable Energy Reviews*, vol. 93, pp. 201-214, Oct. 2018.

[6] Ming Fang, A. I. Gardiner, Andrew MacDougall, and G. A. Mathieson, "A novel series dynamic voltage restorer for distribution systems," in Proc. *IEEE International Conference on Power System Technology*, vol. 1, pp. 38-42, 1998.

[7] Muhammad Mansoor, Norman Mariun, Arash Toudeshki, Noor Izzri Abdul Wahab, Ahmad Umair Mian, and Mojgan Hojabri," Innovating problem solving in power quality devices: A survey based on Dynamic Voltage Restorer case (DVR)," *Journal of Renewable and Sustainable Energy Reviews*, vol. 70, pp. 1207-1216, Apr. 2017.

[8] Abderrahim Telli and Said Barkat, "Distributed grid-connected SOFC supporting a multilevel dynamic voltage restorer," *Journal of Energy Systems*, vol. 10, no. 2, pp. 461-487, May. 2019.

[9] Chunming Tu, Qi Guo, Fei Jiang, Zhikang Shuai, and Xi He, "Analysis and control of bridge-type fault current limiter integrated with the dynamic voltage restorer," *International Journal of Electrical Power & Energy Systems*, vol. 95, pp. 315-326, Feb. 2018.

[10] R. Sitharthan, C. K. Sundarabalan, K. R. Devabalaji, Sathees Kumar Nataraj, and M. Karthikeyan, "Improved fault ride through capability of DFIG-wind turbines using customized dynamic voltage restorer," *Journal of Sustainable cities and society*, vol. 39, pp. 114-125, May. 2018.

[11] Jiangfeng Wang, Yan Xing, Hongfei Wu, and Tianyu Yang, "A novel dual-DC-port dynamic voltage restorer with reduced-rating integrated DC–DC converter for wide-range voltage sag compensation," *IEEE Transactions on Power Electronics*, vol. 34, no. 8, pp. 7437-7449, Aug, 2019.

[12] Talada Appala Naidu, Sabha Raj Arya, and Rakesh Maurya, "Multi objective dynamic voltage restorer with modified EPLL control and optimized pi-controller gains," *IEEE Transactions on Power Electronics*, vol. 34, no. 3, pp. 2181-2192, May 2018.

[13] Jian Ye, Hoay Beng Gooi, Benfei Wang, Yuanzheng Li, and Yun Liu, "Elliptical restoration based single-phase dynamic voltage restorer for source power factor correction," *Journal of Electric Power Systems Research*, vol. 166, pp. 199-209, Jan. 2019.

[14] Nirmalya Mallick and Vivekananda Mukherjee, "Interval type 2 fuzzy logic controlled advanced dynamic voltage restorer for voltage sag alleviation," *IET Generation, Transmission & Distribution*, vol. 13, no. 14, pp. 3020-3028, Apr. 2019.

[15] Neelam Kassarwani, Jyoti Ohri, and Alka Singh. "Performance analysis of dynamic voltage restorer using modified sliding mode

control," *International Journal of Electronics Letters*, vol. 7, no. 1, pp. 25-39, Jan. 2019.

[16] Vu Thai Hung, Hongchun Shu, and Nguyen Duc The, "Double-loop control structure using proportional resonant and sequence-decoupled resonant controllers in static coordinates for dynamic voltage restorer," *Chinese Journal of Electrical Engineering*, vol. 5, no. 3, pp. 10-19, Oct. 2019.

[17] Parag Kanjiya, Bhim Singh and Ambrish Chandra, "SRF theory revisited to control self-supported dynamic voltage restorer (DVR) for unbalanced and nonlinear loads," *IEEE Transactions on Industry Applications*, vol. 49, no. 5, pp. 2330-2340, Oct. 2011.

[18] Hussam M M Alhaj, Nursyarizal Mohd Nor, Vijanth S. Asirvadam and M. F. Abdullah, "Power system harmonics estimation using LMS, LMF and LMS/LMF," in Proc. *IEEE 5th International Conference on Intelligent and Advanced Systems* (ICIAS), pp. 1-5, Jun. 2014.

[19] Manem Srinivas, Ikhlaq Hussain and Bhim Singh, "Combined LMS-LMF based control algorithm of DSTATCOM for power quality enhancement in distribution system," *IEEE Transactions on Industrial Electronics*, vol. 63, no. 7, pp. 4160-4168, Jul. 2016.

[20] J. R. S Martins, D. A. Fernandes, F. F. Costa, M. B. R. Correa, A. J. Sguarezi Filho and E. R. C. da Silva, "Optimized voltage injection techniques for protection of sensitive loads," *International Journal of Electrical Power and Energy Systems*, vol. 116, 105569, March 2020.

[21] Nirmalya Mallick and Vivekananda Mukherjee, "Self-tuned fuzzy-proportional-integral compensated zero/minimum active power algorithm based dynamic voltage restorer," *IET Generation, Transmission & Distribution*, vol. 12, no. 11, pp. 2778-2787, Mar. 2018.

[22] V. John Mathews and Zhenhua Xie, "A stochastic gradient adaptive filter with gradient adaptive step size," *IEEE Transactions on Signal Processing*, vol. 41, no. 6, pp. 2075-2087, Jun. 1993.

[23] R. V. Rao, "Rao algorithms: Three metaphor-less simple algorithms for solving optimization problems,"*International Journal of Industrial Engineering Computations*, vol. 11, no. 1, pp. 107-130. 2020.

Talada Appala Naidu (SM' 18, M'20) received his B. Tech in Electrical and Electronics Engineering from Jawaharlal Nehru Technical University, Kakinada, India, in 2012; and M. Tech and PhD in Electrical Engineering Department from Sardar Vallabhbhai National Institute of Technology, Surat, India, in 2016 and 2020 respectively. He received BEST PAPER AWARD for one of his papers in IEEE conference PETPES-2019 at NIT Suratkal. He has worked as visiting researcher in Khalifa University of Science and Technology, Abu Dhabi after PhD. Currently he is working as Guest faculty in NIT, ANDHRA PRADESH. His fields of interests include applications of power electronics in distribution systems, power quality, Renewable energy sources, and Artificial intellegence.

.

Sabha Raj Arya (M'12, SM'15) received Bachelor of Engineering degree in Electrical Engineering from Government Engineering College Jabalpur, in 2002, Master of Technology in Power Electronics from Motilal National Institute of Technology, Allahabad, in 2004 and Ph.D. degree in Electrical Engineering from Indian Institute of Technology (I.I.T) Delhi, New Delhi, India, in 2014. He is joined as Assistant Professor, Department of Electrical Engineering, Sardar Vallabhbhai National Institute of Technology, Surat. January 2019, he is promoted as Associate Professor in same institute. His fields of interest include Power electronics, power quality, design of power filters and distributed power generation.

He received Two National Awards namely INAE Young Engineer Award from Indian National Academy of Engineering, POSOCO Power System Award from Power Grid Corporation of India in the year of 2014 for his research work. He is also received Amit Garg Memorial Research Award-2014 from I.I.T Delhi from the high impact publication in a quality journal during the session 2013-2014. At present, he has published more than *Hundred* research paper in internal national Journals and conferences in field of electrical power quality.

He also serves as an Associate Editor for the *IET (U.K.) Renewable Power Generation.*

Rakesh Maurya (M'16) received B. Tech in Electrical Engineering from the Kamla Nehru Institute of Technology Sultanpur, Uttar Pradesh in 1998 and M. Tech and Ph.D. in Electrical Engineering from Indian Institute of Technology Roorkee, India in 2002 and 2014 respectively. Presently, he is serving as faculty member in the department of Electrical Engineering, Sardar Vallabhbhai National Institute of Technology Surat, Gujarat, India. His fields of interest include design of Switching Power Converters, High power factor AC/DC Converters, hybrid output converter, Power quality problems, Advanced Electric drives and applications of Real Time Simulator for the control of power converters.

Sanjeevikumar Padmanaban (Member'12–Senior Member'15, IEEE) received the bachelor's degree in electrical engineering from the University of Madras, Chennai, India, in 2002, the master's degree (Hons.) in electrical engineering from Pondicherry University, Puducherry, India, in 2006, and the PhD degree in electrical engineering from the University of Bologna, Bologna, Italy, in 2012. Hewas an Associate Professor with VIT University from 2012 to 2013. In 2013, he joined the National Institute of Technology, India, as a Faculty Member. In 2014, he was invited as a Visiting Researcher at the Department of Electrical Engineering, Qatar University, Doha, Qatar, funded by the Qatar National Research Foundation (Government of Qatar). He continued his research activities with the Dublin Institute of Technology, Dublin, Ireland, in 2014. Further, he served an Associate Professor with the Department of Electrical and Electronics Engineering, University of Johannesburg, Johannesburg, South Africa, from 2016 to 2018. Since 2018, he has been a Faculty Member with the Department of Energy Technology, Aalborg University, Esbjerg, Denmark. He has authored over 300 scientific papers.

S. Padmanaban was the recipient of the Best Paper cum Most Excellence Research Paper Award from IET-SEISCON'13, IET-CEAT'16, IEEE-EECSI'19, IEEE-CENCON'19 and five best paper awards from ETAEERE'16 sponsored Lecture Notes in Electrical Engineering, Springer book.